Rearrangement of twin variants in ferromagnetic shape memory alloy–polyurethane composites studied by stroboscopic neutron diffraction



2008 J. Phys.: Condens. Matter 20 104247

(http://iopscience.iop.org/0953-8984/20/10/104247)

IOP Publishing Journal of Physics: Condensed Matter

J. Phys.: Condens. Matter **20** (2008) 104247 (5pp) doi:10.1088/0953-8984/20/10/104247

# Rearrangement of twin variants in ferromagnetic shape memory alloy–polyurethane composites studied by stroboscopic neutron diffraction

**J Feuchtwanger[1], P Lázpita[1], N Vidal[1], J M Barandiaran[1], J Gutiérrez[1], T Hansen[2], M Peel[3,6], C Mondelli[4], R C O'Handley[5] and S M Allen[5]**

[1] Facultad de Ciencia y Tecnología, Departamento Electricidad y Electrónica, Universidad del Pais Vasco UPV/EHU, PO Box 644, E-48080 Bilbao, Spain
[2] Institut Laue-Langevin, 6 Rue Jules Horowitz, F-38042-Grenoble Cedex 9, France
[3] FaME38 ILL-ESRF, 6 Rue Jules Horowitz, F-38042-Grenoble Cedex 9, France
[4] CNR-INFM and CRS-SOFT, Institute Laue-Langevin, 6 Rue Jules Horowitz, F-38042-Grenoble Cedex 9, France
[5] Department of Materials Science and Engineering, Massachusetts Institute of Technology, Cambridge, MA 02139, USA

E-mail: bcpfemoj@ehu.es (J Feuchtwanger)

Received 16 July 2007, in final form 3 December 2007
Published 19 February 2008
Online at stacks.iop.org/JPhysCM/20/104247

**Abstract**

The use of ferromagnetic shape memory alloy (FSMA) particles as fillers in polymeric matrix composites has been proposed for vibration damping. The large pseudo-plastic recoverable deformation of the FSMA particles due to the rearrangement of twin variants can dissipate a large amount of energy, both under compression and tension. The composites studied are made by mixing particles of NiMnGa with a polyurethane matrix. A magnetic field is applied to the composite while the matrix sets, to achieve a strong [112] texture in the field direction. *In situ* strobed neutron diffraction measurements were carried out while the composites were subjected to a cyclic deformation. They show that the intensity of certain peaks varies during the deformation cycle. All the peaks that show this behavior can be grouped into pairs that stem from a single austenitic peak. The (020) and (112) martensite peaks correspond to the splitting of the (220) austenite peak, and the intensity of one increases as that of the other decreases. The neutron measurements show directly that there is a change in the texture of the composite during the stress cycle applied to the composite and confirm that the large mechanical loss observed in the stress–strain cycles is in good part due to the rearrangement of twin variants in the FSMA filler used in the composites.

(Some figures in this article are in colour only in the electronic version)

## 1. Introduction

The use of ferromagnetic shape memory alloy (FSMA)/ polymer composites for mechanical energy absorption has already been proposed and encouraging results have been shown [1–3]. It is well known that the large magnetic field induced strain observed in these alloys is due to the motion of twin boundaries, and it has been shown that both a magnetic field as well as an external stress can cause the motion of those twin boundaries. Twin boundary motion is seen in the stress–strain plots as a pseudo-plastic deformation, and most of the energy deforming the material is not given back by the system

[6] Present address: Institute Laue-Langevin, Grenoble, France.

 

when the load is removed, leading to a large amount of energy dissipated every cycle. Unlike plastic deformation, pseudo-plastic deformation can be fully recovered and the material can be returned to its starting configuration by applying a stress in the opposite direction, allowing for cyclic deformation. The same large (6%) deformation can be obtained repeatedly for several thousands of cycles [4]. This large ability to dissipate mechanical energy makes these alloys ideal for vibration damping applications. In addition the large magneto-crystalline anisotropy [5], crucial for their use as magnetic actuators, makes it possible to obtain textured composites. When a magnetic field is applied to the FSMA/polymer slurry during the curing, the particles will align into chains to minimize the magneto-static energy of the composite, and they will also orient so that the easy-axis of magnetization of the particles will be parallel to the applied magnetic field. The result is a composite with a pseudo 3:1 connectivity, and the orientation of the particles maximizes the resolution of the stress applied along the chain direction as a shear on the twin planes, favoring their motion.

As has already been shown, applying a load to these composites can cause a reorientation of the twin variants, this was determined under static conditions, indirectly through magnetic measurements [1, 6, 7] and directly through x-ray diffraction measurements [8]. It has also been speculated that the twin boundaries can reorient dynamically since these composites show large mechanical losses when cyclic loads are applied to them, and the corresponding stress–strain plots show features indicative of twin motion [9].

## 2. Experimental details

### *2.1. Sample preparation*

Composite samples used for the experiments were prepared by mixing spherical particles 25–75 $\mu$m in diameter of Ni–Mn–Ga (nominal composition: Ni 50.4 at.%, Mn 29.9 at.% and Ga 19.7 at.%) made by spark erosion under liquid argon, as described in [10], with a commercial two-part room temperature curing polyurethane made by Lord® Corporation. The Ni–Mn–Ga particles used are reported to be a tetragonal martensite with lattice constants $a = 5.932$ Å and $c = 5.584$ Å, this corresponds to a $\frac{c}{a}$ ratio of 0.94 [11]. The mass ratios of the polymer and the FSMA filler were chosen to achieve a 25% by volume FSMA in the composite once the matrix cured. The uncured slurry was poured into a polytetrafluoroethylene mold that contained two aluminum end-caps with a dovetail cavity connected to a straight throat by rounded corners that fed into the main cavity of the mold. The end-caps were separated by a rectangular prism section that made up the main cavity of the mold, 5 mm × 5 mm × 10 mm in dimensions. The samples were clamped afterwards by the aluminum end-caps to prevent the sample from slipping out of the grips while in tension due to the lateral shrinkage. After the mold was filled it was placed into an electromagnet and a 0.5 T field was applied to the sample along the long direction of the prism while the polymer cured. The only variation in the preparation of the composite samples from those used in previous publications [1, 2], is a redesign of the end-caps to minimize stress concentration points.

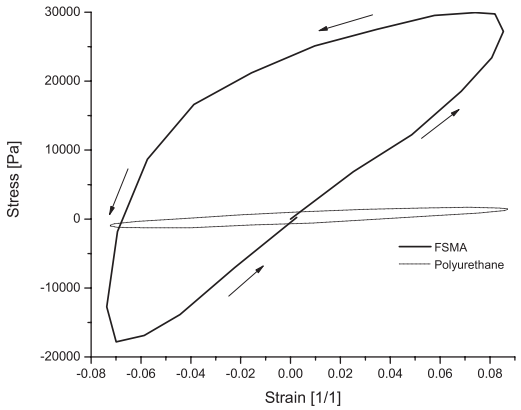


**Figure 1.** Stress versus strain plot for the polyurethane matrix (dashed trace) and for a 25 vol% FSMA loaded composite (solid trace). The arrows show the direction of loading.

### *2.2. Neutron diffraction measurements*

The neutron diffraction experiments were carried out on the D20 diffractometer ($\lambda = 1.87$ Å) at the Institute Laue-Langevin in Grenoble, France. A hydraulically driven mechanical testing machine, custom built by Instron®, was mounted inside the diffractometer. The neutron beam was shaped by the Cd shielding on the grips of the mechanical testing machine; as a result, only the sample area was covered by the beam. The mechanical load was applied along the particle chain direction, which corresponds to the [112] direction in the particles, and the neutron beam incident on the sample was in the isotropic plane normal to the sample texture direction.

The mechanical testing machine was set to run under strain control mode, and the analog strain output form the Instron® 8800 control unit was used to trigger a pulse generator to produce the 5 V TTL signal needed to synchronize the mechanical testing cycles to the spectra acquisition. Stress and strain data collected during the experiment was saved on the computer that controlled the mechanical testing machine. For all the experiments a 0.5 Hz sinusoidal drive was used, the amplitude of the drive strain was 0.8 mm peak-to-peak, this corresponded to an 8% strain on the sample.

The neutron diffraction data were collected in stroboscopic mode, and were triggered by the TTL signal generated from the strain output signal. The strobed mode consisted of taking 100 slices of 20 ms each, after each trigger event, covering one full mechanical deformation cycle. Data were collected over several cycles and corresponding slices from all cycles were added to obtain a larger number of counts.

Additionally, diffraction spectra were collected on the samples under static tensile and compressive loads.

## 3. Results

The stress–strain plot for the FSMA composite in figure 1 (labeled FSMA) shows a much larger hysteresis than the

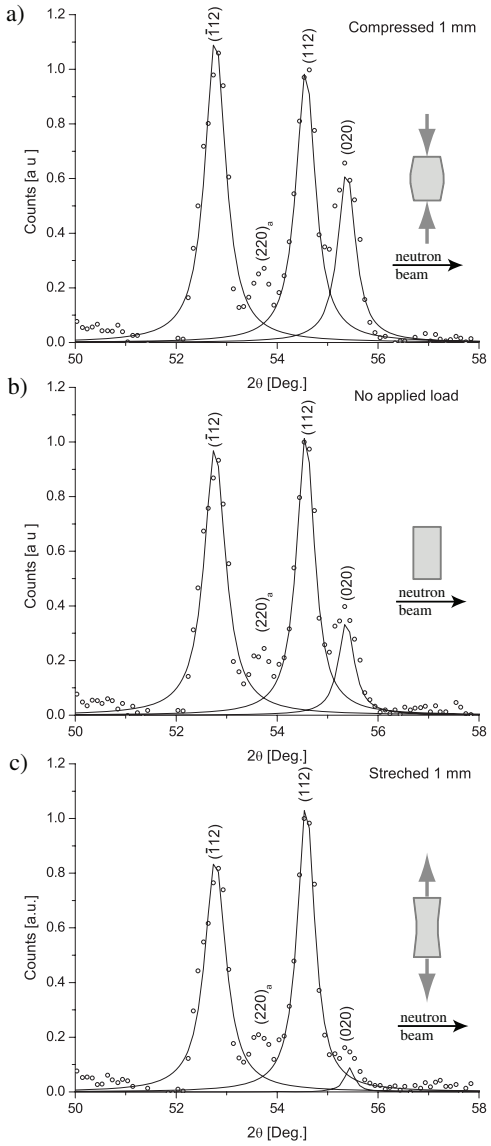


**Figure 2.** Normalized static neutron diffraction pattern for (a) the composite compressed 1 mm under a tensile load, (b) under no load and (c) stretched 1 mm. Open circles correspond to the experimental diffraction data, solid lines correspond to the fitted Lorentzian peaks. The $(220)_a$ corresponds to retained austenite.

matrix polymer with no filler (labeled polyurethane). The polyurethane matrix with no filler (dotted line) shows the typical elliptical stress–strain plot for a viscoelastic material. In contrast, the plot for the FSMA loaded composite (solid line) deviates drastically from ellipticity. It shows three distinct slopes throughout the cycle. When comparing both plots on the graph it can be seen that for the same strain amplitude, the stress amplitude for the composite is much larger, and that the area contained within the plot is considerably larger than that for the unloaded polymer. The area within the cycle is the energy dissipated per tension–compression cycle.

Figure 2 shows the neutron diffraction pattern for a 25% by volume FSMA composite under three different load conditions. The composite deformed 1 mm under tensile load shows two clear peaks, at about 52.5° ($\bar{1}12$) and 54.5° (112), a

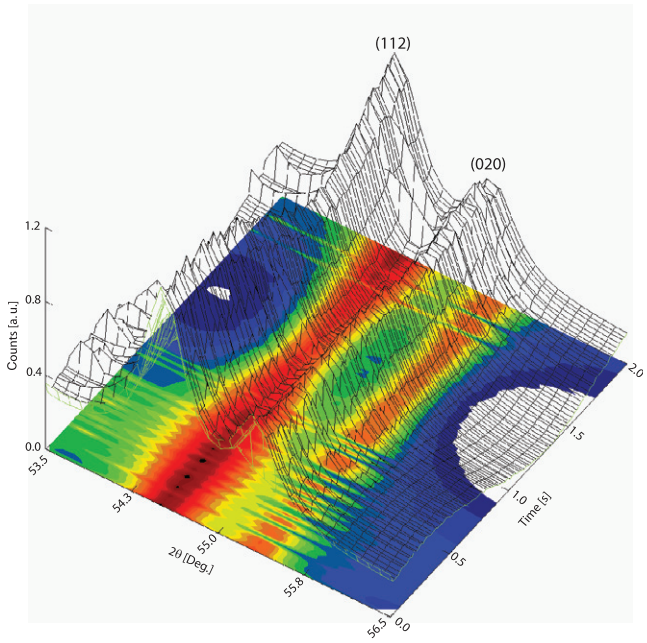


**Figure 3.** Three-dimensional (3D) plot showing the intensity as a function of time and angle for the (112) and (020) peaks.

faint third peak can be seen near 55.5° (020) (figure 2(c)). As the load transitions from tensile to compressive, the relative intensity of the peak at 55.5° (020) increases and becomes clearly visible for the sample under no load. For the composite under a compressive load, the intensity of the peak at 55.5° (020) grows drastically and becomes comparable to that of the other peaks in the plot. The area ratio for the peak at 55.5° (020) to the one at 54.5° (112) for the sample under tension is 0.05, while the ratio for the same peaks in the sample under compression is 0.57. The area ratio for the sample under no stress is 0.29. While the particle manufacturer reported the particles as being tetragonal martensite, the peaks we found to show the stress-induced changes in intensity corresponded to orthorhombic martensite. All the indexes reported correspond to the martensite cell, which is rotated 45° about the *c*-axis.

Figure 3 shows the diffraction pattern under strobed conditions for the composite while being subjected to a 0.08 strain amplitude. The angle range was chosen to only include the peak that showed the largest variation in the static measurements, the (020) and (112) peaks. The crystallographic relation these peaks hold to each other will be described in the discussion. It should be noted that the intensity of the (112) peak shows a variation in intensity as a function of time while the (020) peak shows no apparent variation. The apparent relation between the background and the peaks becomes irrelevant when their ratio is calculated for each slice, because the background is subtracted and does not contribute to the area of each peak.

The ratio of the area of the (020) peak to the area of the (112) peak, as a function of time, is shown in figure 4. No smoothing was performed on the data presented. The peak areas were obtained by fitting the peaks to Lorentzians, with the background subtracted at each time slice. The area ratio shows a trend that resembles a sinusoid, but as can be seen

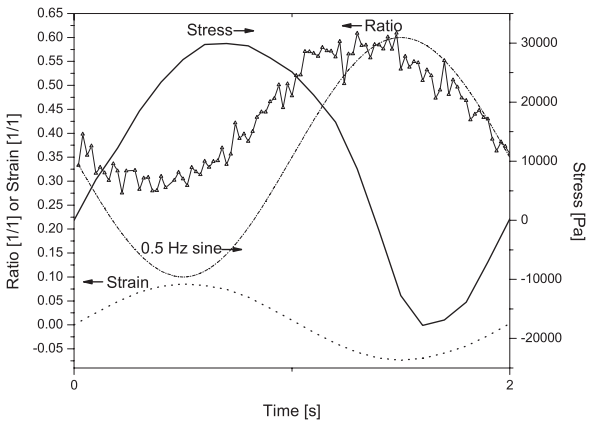


**Figure 4.** Area ratio for the (020) to the (112) peaks, strain and stress on the composite as a function of time for a 25 vol% FSMA composite as a function of time. A 0.5 Hz sine wave (dashed line) is plotted along with the area ratio for illustrative purposes.

by comparing with the sine wave plotted on the same graph (dashed line), it does not exactly match. The 'zero crossing' for the area ratio plot is shifted from the midpoint and the amplitude is asymmetric about the horizontal line that connects the two endpoints of the area ratio plot. Stress and strain as functions of time are shown below, plotted so that the time scales for all plots correspond. The strain is sinusoidal as should be expected since the experiment was carried out under strain control mode. The stress, however, shows a curve that is not purely sinusoidal and shows a broad tensile upper half and a narrower compressive lower half. The ratio of the $(\bar{1}12)$ to the (112) peak showed no change as a function of time.

## 4. Discussion

The stress–strain plot for the polymer with no filler is perfectly elliptical, this indicates that the stress resulting from a sinusoidal stress is also sinusoidal, but lags the drive. This is the result of the loss being only due to a viscous drag. Conversely the stress–strain plot for the FSMA loaded composite departs drastically from ellipticity, hinting at an additional loss mechanism at work in the composite. Additional loss due to an inert filler would cause a greater phase lag between the stress and the strain, but it would not account for the additional features observed in the stress–time plot. The difference in behavior under loading and unloading is the result of the load being transferred more efficiently in the compressive part of the cycle than in the tensile one. This is to be expected since the curing of the composite under a magnetic field yields a pseudo 3:1 composite, with discontinuous particle chains in the load direction. Under compression the particles push against each other transferring the load better than under tensile loading, where the particles separate and the load is transferred through a polymeric matrix, through the Poisson effect by the polymer surrounding the particles and direct traction along the stress axis by the polymer linking the particles axially.

The stress–strain plot in figure 1 is traced in a counter-clockwise direction, starting at the lowest point, as the composite is stretched stress in the matrix builds up and slowly transmits to the particles. The twin boundaries move gradually as their individual threshold stress is reached. The modulus is dominated by the polymer matrix, resulting in the constant slope observed. Once the crest is reached the strain direction reverses and the particles start pushing against each other, stress builds up more rapidly until the threshold stress for twin motion is reached, the particles yield and the sharp drop in stress is observed.

The relative change in intensity for the peaks observed in figure 2 becomes relevant when the area ratio for the peak at 55.5° to the one at 54.5° is taken. These peaks correspond to the (020) and the sum of the (112) and $(\bar{1}\bar{1}2)$ respectively, indexed in the martensite, and are the result of the splitting of the (220) austenite peak upon phase transition into the martensite. The (112) and $(\bar{1}\bar{1}2)$ peaks are two equivalent orthogonal peaks that show up at the same angle and their individual contributions cannot be measured individually. The change in relative intensities can only be explained by a change in the relative number of (020) planes with their normal parallel to the neutron beam at the expense of the (112) or $(\bar{1}\bar{1}2)$ planes. Whether the (020) grows at the expense of the (112) or $(\bar{1}\bar{1}2)$ depends on the orientation of the twin planes that form when the material initially transforms into the martensite. The stress-induced rotation of the (020) into the beam direction is explained by the stress-induced growth of a twin variant at the expense of another one through twin motion. It could be argued that the change in relative amplitudes of the peaks could be attributed to a physical rotation of the particles in the composite, but this is very unlikely and can be ruled out for several reasons: first of all, the particles used were mostly spherical, this means there is no geometrically preferred orientation for the particles in the composite when a load is applied to it as would be the case with needle-like particles. Secondly, the tilting of the particle chain axis due to the bowing of the sample under stress is very small, and can be approximated to be at maximum 5° for the chains near the edge of the composite by a simple trigonometric calculation. That also indicates that if the particles had delaminated and were free to rotate within the matrix, the rotation due to the applied stress would only be of the order of a few degrees and could not account for the drastic change observed. Lastly, particle rotation would not be consistent over 2000 cycles, while the change observed is.

Figure 4 shows that the same variation in area ratios for the (020) to the sum of the (112) and $(\bar{1}\bar{1}2)$, which are crystallographically identical, observed in figure 2, but under dynamic conditions. The sinusoidal-like behavior observed cannot be attributed to the background modulation observed in figure 3 since the area ratios are a relative measurement that is independent of adjacent slices, unlike the background amplitude that follows the strain. The beam intensity changes because the size of the window for the beam is given by the distance between sample grips, which is the strain on the sample.

The change in the area ratio of the (020) to the (112), which are orthogonal to each other while the composite maintains the same orientation to the neutron beam, can only

be explained by twin boundary motion. Additionally, change in ratio tracks the change in stress, but cannot be attributed to the change in intensity of the background, since it is inherently a relative measurement and the background is subtracted at each slice when the areas are fitted. Given the sample size and the filling factor of the composite, the amount of material diffracting the neutron beam was small, the number of counts that each individual cycle yielded was also small. This meant that a lot of cycles had to be measured to obtain a good statistic for each slice. Unfortunately the matrix failed after only approximately 2000 cycles (or 40 s of data collection at each slice) which resulted in data clean enough to make out a clear trend, but not clean enough to make a quantitative assessment of the sharpness of the transitions in the area ratio variation. Without a clear picture of the breadth of the transition it is not possible to determine the width of the variation in threshold stresses for the particles, be this due to compositional inhomogeneities or misorientation of the particles relative to the stress axis.

The point where the tensile stress reaches a maximum (about 0.03 MPa) corresponds with the start in the increase in the area ratio, and the increase continues while the stress remains above about 0.018 MPa. The area ratio then remains constant until the stress reaches a minimum (about −0.018 MPa) at which the area ratio begins to decrease again. These features match the features on the stress–strain curve for the composite shown in figure 1, the flat region at the top of the stress–strain plot corresponds to the region where the area ratio increases, indicating a connection between the high mechanical loss observed and the twin boundary motion in the FSMA filler material.

## 5. Conclusions

The change in the area ratio of the (112) to the (020) can only be explained by the change in the twin variant distribution. Twinning is the only mechanism that appropriately explains a change in texture in the composite where the (112) planes go from being normal to the particle chain direction to containing the particle chain direction and in doing so change their orientation to the neutron beam by 90°. The stress on the composite as a function of time shows a marked departure from a sine function, even though the drive was controlled to be a sine wave. This shows that there is a change in the modulus of the composite which is repeatable from cycle to cycle. The matrix material did not show this behavior, it showed a constant modulus. The pseudo-plastic deformation of the particles due to variant reorientation observed in neutron diffraction accounts for the change in stiffness of the composite. This demonstrated plastic deformation of the filler material can account for a fair fraction of the increased loss per unit volume of material observed in these composites.

## Acknowledgments

JF would like to acknowledge the financial support of the EU Marie Curie IIF actions under FP6. This work has been performed under the financial support of the ACTIMAT project funded by the Basque Government's Department of Industry and the ONR's MURI Project grant N00014-01-10758. We thank FaME38 ILL-ESRF and are especially grateful to Darren Hughes for the use of the mechanical testing machine.

## References

[1] Feuchtwanger J, Michael S, Huang J K, Bono D, O'Handley R C, Allen S M, Jenkins K, Goldie J and Berkowitz A 2003 Energy absorption in Ni–Mn–Ga polymer composites *J. Appl. Phys.* **93** 8528–30

[2] Feuchtwanger J, Griffin K, Huang J K, O'Handley R C, Allen S M and Bono D 2003 Vibration damping in Ni–Mn–Ga-polymer composites *Proc. SPIE* **5052** 92–7

[3] Gans E, Henry C and Carman G P 2004 High-energy absorption in bulk ferromagnetic shape memory alloys ($Ni_{50}Mn_{29}Ga_{21}$) *Proc. SPIE* **5387** 177–85

[4] Heczko O, Straka L L, Soderberg O and Hannula S 2005 Magnetic shape memory fatigue *Smart Struct. Mater; Proc. SPIE* **5761** 513–20

[5] Straka L and Heczko O 2003 Magnetic anisotropy in Ni–Mn–Ga martensites *J. Appl. Phys.* **93** 8636–9

[6] Feuchtwanger J, Griffin K, Huang J K, Bono D, O'Handley R C and Allen S M 2004 Mechanical energy absorption in Ni–Mn–Ga polymer composites *J. Magn. Magn. Mater.* **272–276** 2038–9

[7] Scheerbaum N, Hinz D, Gutfleisch O, Mueller K-H and Schultz L 2007 Textured polymer bonded composites with Ni–Mn–Ga magnetic shape memory particles *Acta Mater.* **55** 2707–13

[8] Scheerbaum N, Hinz D, Gutfleisch O, Skrotzki W and Schultz L 2007 Compression-induced texture change in NiMnGa–polymer composites observed by synchrotron radiation *J. Appl. Phys.* **101** 09C501

[9] Feuchtwanger J, Richard M L, Tang Y J, Berkowitz A E, O'Handley R C and Allen S M 2005 Large energy absorption in Ni–Mn–Ga/polymer composites *J. Appl. Phys.* **97** 10M329

[10] Solomon V C, McCartney M R, Smith D J, Tang Y, Berkowitz A E and O'Handley R C 2005 Magnetic domain configurations in spark-eroded ferromagnetic shape memory Ni–Mn–Ga particles *Appl. Phys. Lett.* **86** 192503

[11] Tang Y J, Smith D J, Hu H, Spada F E, Harper H and Berkowitz A E 2003 Spark-eroded particles: influence of processing parameters *IEEE Trans. Magn.* **39** 3405–7